ACS Biomaterials SCIENCE & ENGINEERING

pubs.acs.org/journal/abseba
Article

Biogenesis of Au Nanoparticles from Plant-Derived Metabolites – *In Vitro* and *In Vivo* Studies

Julia Kulczyńska, Natalia Topa, Magdalena Widziołek, Joanna Homa, Inga Kwiecień, Enrique Gamez, Manuel Arruebo, and Agnieszka Kyzioł*

Cite This: *ACS Biomater. Sci. Eng.* 2026, 12, 1508–1521

ABSTRACT: Biomimetic gold nanoparticles (Au NPs) were synthesized via a sustainable approach without any additional toxic chemical reagents and fully characterized. It was proven that only whole aqueous extracts of *Rosa damascene* (RD) and *Rosa rugosa* (RR) are powerful enough to reduce, graft, and stabilize metallic nanostructures, resulting in the formation of stable, monodisperse nanocolloids (Au@RD NPs and Au@RR NPs) whereas individual constituent molecules were insufficient to yield stable metal NPs. The biological study conducted, both *in vitro* and *in vivo*, revealed no acute cytotoxicity (in HaCaT cell lines and zebrafish larval models) but bacteriostatic activity at equivalent doses with potent inhibition of biofilm formation (for a MRSA strain). Noteworthy, the additive antibacterial activity of rose extracts when combined with rifampicin promotes that these attractive inorganic−organic hybrids could be suitable alternatives to combat the acquisition of antimicrobial resistance. This huge application potential was also emphasized by the presence of insignificant changes in the expression of pro-inflammatory cytokine genes (*IL-1β*, *IL-6*, and *CXCL8*) and apoptotic/autophagic associated genes (*TP53*, *MAP1LC3B*, and *SQSTM1*) in treated HaCaT cells at antimicrobial doses. In addition, at the studied doses, the survival of *Danio rerio* larvae and their proper development (i.e., lack of deformities) endorsed biocompatibility *in vivo*.

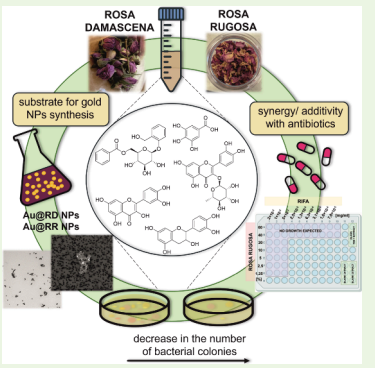

KEYWORDS: *polyphenols, plant extracts, Au nanoparticles, biocompatibility, antimicrobial activity, biofilm inhibition*

1. INTRODUCTION

The emergence of antibiotic-resistant strains, attributed to the widespread overuse of antibiotics, resulted in antimicrobial resistance (AMR) that is currently a major global problem.[1] An urgent necessity in the present alarming situation is to search for new and effective solutions to not only prevent and combat the growing AMR but also identify effective bactericidal agents having multiple mechanisms of action that can be safely and widely used.

A promising group of drugs with antimicrobial potential is those based on natural products. Data on the marketing of small-molecule antimicrobial drugs show a significant advantage of natural products and their derivatives (70.6%) over synthetic drugs (28.6%).[2,3] In this context, plant metabolites, known by their ability to target microbial cell membranes, interfere with the synthesis of microbial DNA/RNA/enzymes and disrupt quorum sensing and efflux pump expression are considered as powerful candidates for the development of novel natural antimicrobial agents.[4,5] Folk medicine has recognized the therapeutic potential of extracts from two species of rose − damask rose (*Rosa damascena,* RD) and rugosa rose (*Rosa rugosa,* RR) − for treating stomachaches, headaches, coughs, healing wounds, relieving nervous tension, and improving mood. In general, their medicinal effects are attributed to the presence of polyphenols, which exhibit antibacterial, antioxidant, anti-inflammatory, antidepressant, anticancer, and free radical scavenger activities.[6−11]

On the other hand, significant progress has recently been made discovering other approaches to overcome AMR, for instance, the use of composite metallo-antimicrobials. Their possible modes of action are categorized into different classes: inhibitors of enzymes, membrane perturbants/disruptors, inhibitors of uptake/efflux pumps, inhibitors of biofilm formation and quorum sensing (persister inhibitors), and oxidative inducers.[12,13] Noteworthy, the functionalization of the surface of nanomaterials with natural compounds (e.g., polyphenols) can enhance their cellular uptake.[14−16] In the present study, polyphenols present in rose extracts were used as reducing and stabilizing agents for the synthesis of gold nanoparticles (Au NPs), which is a process also aligned with the principles of sustainable chemistry. Furthermore, the advantage of such synthesized NPs using natural sources is that they generally exhibit lower toxicity than their chemically

Received: August 25, 2025
Revised: December 28, 2025
Accepted: December 30, 2025
Published: February 4, 2026

https://doi.org/10.1021/acsbiomaterials.5c01488
ACS Biomater. Sci. Eng. 2026, 12, 1508−1521

synthesized counterparts.[17] Au NPs, despite their lower antimicrobial activity compared to the widely described Ag NPs,[18] constitute optimal carriers for drugs or antibodies due to their biocompatibility, low toxicity, easy surface functionalization, or photothermal activity.[19] Au NP antimicrobial mechanisms are based on the following: (i) the alteration of the cellular membrane potential and the inhibition of ATP synthase, with a consequent decrease in ATP levels and impaired metabolism, (ii) the inhibition of the ribosome subunit capable of binding tRNA, which adversely affects protein synthesis,[20] (iii) the influence on the process of chemotaxis, which involves the use of transmembrane signal transducers produced by bacteria to respond to changes in the chemical composition of the surrounding environment,[21] and (iv) a ROS-independent mechanism of action due to Au NPs' chemical inertness (likewise some antibiotics e.g., aminoglycosides) ensuring low toxicity to mammalian cells.[22]

Importantly, any novel strategy based on multitargeted mechanisms due to multicomponent hybrids offers significant advantages over a unicursal approach and renders less likelihood to generate resistance. Thus, proposing novel metallo-drugs as unique systems combining metal nanocarriers and bioactive plant extracts optimizes their administration route, increasing the selectivity by achieving a multitarget-oriented delivery and minimized side effects. The novelty of this scientific approach fits into the current strategy of investigating novel nanoantibiotics. This Account presents characteristics and novel biomedical applications of rose extracts and gold NPs. Their synthesis and physicochemical properties are described together with an evaluation of their antibacterial and antibiofilm activity and a preliminary assessment of their mechanism of antimicrobial action. In addition, toxicological studies were performed to evaluate their safety *in vitro* on HaCaT cells and *in vivo* on zebrafish larvae (*Danio rerio*) to determine a tolerable concentration allowing their safe use in antimicrobial applications.

2. MATERIALS AND METHODS

2.1. Materials

Plant material (*Rosa damascena* buds and *Rosa rugosa* petals; origin: Bulgaria) was purchased from Kosmetyki z Doliny Róż (Ząbki, Poland). Tetrachloroauric(III) acid trihydrate ($HAuCl_4{\cdot}3H_2O$) and rifampicin (RIF, ≥ 97%) were provided by Merck (Darmstadt, Germany). Tryptone soy broth (TSB) was supplied by Laboratorios Conda-Pronadisa SA (Madrid, Spain), and tryptone soy agar plates (TSA) were purchased from Avantor VWR (Radnor, PA, USA). Fetal bovine serum (FBS), Dulbecco's modified Eagle medium (DMEM), and Trypsin-EDTA solution were obtained from Corning (New York, USA). For RNA isolation, the Universal RNA Purification Kit from EUR_X (Gdańsk, Poland) was used. Moreover, the TranScriba Kit was supplied by A&A BIOTECHNOLOGY (Gdańsk, Poland). Starters for PCR reaction were purchased from Genomed S.A. (Warszawa, Poland) and Sybr Select Master Mix from ThermoFisher (Waltham, USA).

2.2. Preparation of Rose Extracts

To prepare rose extracts, 60 mL of distilled water was heated to 40 °C on a magnetic stirrer. Subsequently, 1.8 g of crushed plant material, depending on the synthesis (RD buds or RR petals), was placed into the water. The material was left for 1 h under stirring and then it was filtered through filter paper and then through a cellulose syringe filter with a pore cutoff of 0.22 μm. Fresh aqueous RD and RR extracts were used for antibacterial and antibiofilm assays immediately after extraction and filtration. For this reason, concentrations in these assays are expressed as % (v/v). Meanwhile, cytotoxicity assays were carried out using extracts dried at 60 °C, for which dry mass was accurately determined, and the concentrations are reported in mg/mL.

2.3. Characterization of Rose Extracts

The characterization of aqueous rose extracts obtained from RD buds and RR petals was carried out by measuring UV−vis spectra of 100-fold dilutions by UV−vis spectrophotometry (Shimadzu 1900, Shimpol). The absorbance maximum at a wavelength of approximately 350 nm was determined. Precise determination of organic compounds, both qualitative and quantitative, was carried out in collaboration with the Department of Medicinal Plant and Mushroom Biotechnology of Jagiellonian University (Poland). The dried samples were dissolved in water at 40 °C to obtain a total mass concentration of 30 mg/mL. The determination was carried out for 90 min in a methanol gradient of 20−100% on a Merck-Hitachi chromatograph equipped with a Purospher RP-18e, 5 μm, 4 × 250 mm analytical column and a DAD detector. Qualification and quantification analysis were based on a comparison with 76 reference substances (Supporting Information: Section S1. *List of analytical standards for HPLC quantification*). The following abbreviations were used: RD − *Rosa damascena* extract from buds, RD* − *Rosa damascena* extract from petals, and RR − *Rosa rugosa* extract from petals.

2.4. Synthesis of Au@RD NPs and Au@RR NPs

Synthesis of Au@RD NPs and Au@RR NPs was carried out according to the previously reported protocol for Au@RD NPs.[23] In brief, a round-bottomed flask containing 16 mL of distilled water and 2 mL of a solution of $HAuCl_4{\cdot}3H_2O$ (5 mM, 2 mL) was placed on a magnetic stirrer (90 °C, 900 rpm). When the substrates had reached the appropriate temperature, the solutions of RD or RR extracts (20 mg/mL, 1 mL), heated to 90 °C, were vigorously poured into the flask, keeping the temperature of the synthesis constant and the vessel protected from light. The immediate appearance of red color indicated the formation of Au NPs: Au@RD NPs and Au@RR NPs, respectively. After 2h, the obtained solution was transferred to a falcon, protected from light, and stored at room temperature or dried at 60 °C in 2 mL eppendorfs. Those Au@RD NPs and Au@RR NPs were then synthesized via a one-step process employing rose-derived extracts, which acted simultaneously as reducing and capping agents. Consequently, NPs devoid of these rose-derived reducing and stabilizing components could not be synthesized to serve as bare controls. Although alternative reducing and capping agents could be utilized (e.g., sodium citrate, ascorbic acid, sodium borohydride, THPC, glucose, CTABr, *etc.*), their resulting physicochemical properties would differ substantially, precluding an unbiased comparison.

2.5. Characterization of Au@NPs

UV−vis spectra of Au@RD NPs or Au@RR NPs colloids after 30, 60, and 120 min were measured to follow the progress of the Au(III) ion reduction. The morphology of the Au NPs was visualized using transmission electron microscopy (TEM, JEOL JEM2100 HT CRYO LaB_6). Based on the microscope images, the particle size was determined using ImageJ software, and then size distribution was analyzed by Origin Pro 2020. Additionally, the hydrodynamic diameter and zeta potential at acidic pH were determined by dynamic light scattering (Nanosizer Ultra, Malvern).

2.6. Antimicrobial Activity of Extracts, Nanoparticles, and Rifampicin

Methicillin-resistant *Staphylococcus aureus* strain (USA300 MRSA, kindly donated by Cristina Prat-Aymerich PhD, MD, from IGTP, Badalona, Spain) was inoculated in 5 mL of TSB and incubated overnight at 37 °C with shaking. The culture was subsequently diluted in fresh TSB to achieve a consistent OD_{600} (≈10^7 colony-forming units, CFU/mL) and transferred to a 96-well plate. Bacterial suspensions (at a concentration of 10^5 CFU/mL) were exposed to varying concentrations of rose extracts (RD, RR; 40−80% v/v), Au NPs (Au@RD NPs, Au@RR NPs; 0.2−1 mg/mL), and rifampicin (0.005−0.05 μg/mL) in TSB followed by incubation at 37 °C for 24

https://doi.org/10.1021/acsbiomaterials.5c01488
ACS Biomater. Sci. Eng. 2026, 12, 1508−1521

h with shaking. The antibacterial activity was assessed via the serial dilution method and subsequent plating of the treated samples on TSA plates. The experiments were performed three times in triplicate, with the results compared with those obtained for untreated control samples.

To identify additive and synergetic effects, the fractional inhibitory concentration index (FICI) was determined for selected samples. Appropriate dilutions of the test compounds were prepared in a 96-well plate: RR extract (3/2 × MIC, MIC, 1/2 × MIC, 1/4 × MIC, 1/8 × MIC, 1/16 × MIC, 1/32 × MIC) and rifampicin (4 × MIC, 1/2 × MIC, 1/4 × MIC, 1/8 × MIC, 1/16 × MIC, 1/32 × MIC, 1/64 × MIC). Each well was inoculated with 10^5 CFU/mL, and then the plate was placed in an incubator at 37 °C for 24 h. After this time, the absorbance was measured at 570 nm by using a Varioskan LUX microplate reader (Thermo Fisher Scientific). Fractional inhibitory concentration index (FICI) values were determined by assessing the transparency of wells (transparent vs turbid) according to the experimental scheme and concentration ranges described for the pair of antimicrobial agents. Complete MIC combination matrices and detailed interpretation rules are provided in the Supporting Information (Section S9. *Fractional inhibitory concentration index (FICI)*: Figure S6). The results were interpreted using the following formula:

$$\mathrm{FICI} = \mathrm{FIC\ A} + \mathrm{FIC\ B} = \frac{\mathrm{MIC\ A(in\ presence\ of\ B)}}{\mathrm{MIC(A)}} + \frac{\mathrm{MIC\ B(in\ presence\ of\ A)}}{\mathrm{MIC(B)}} \quad (1)$$

where A and B are the biologically active tested compounds.

The results were analyzed assigning the following values: synergy, FICI ≤ 0.5; additivity, 0.5 < FICI ≤ 1; no interaction, 1 < FICI ≤ 4; antagonism, FICI > 4.

2.7. Biofilm Growth Inhibition Assay

Dried samples of rose extracts were redissolved in bacteria culture medium (TSB) to achieve a final extract concentration of 300% (v/v) (samples were concentrated to add the minimum amount of water). Colloids were centrifugated (13,000 rpm, 10 min) and solvent was substituted for TSB to have an adequate medium for bacterial growth and to adjust colloids concentration. After centrifugation and resuspensions, colloids were resuspended without observable aggregation.

MRSA bacterial strain was inoculated in 5 mL of TSB and incubated at 37 °C under shaking overnight. After this time, OD_{600} was checked and bacteria concentration was adjusted to 10^7 CFU/mL in 96-well plates with fresh TSB and with the corresponding concentration of the tested extract or gold nanoparticles (RD extract, 7.5−60% v/v; RR extract, 5−40% v/v; Au@RD NPs, 0.20−1.20 mg/mL; Au@RR NPs, 0.25−1.50 mg/mL). Samples were incubated for 24 h at 37 °C without shaking. Plates were kept in a closed box with a constant level of humidity (to avoid water evaporation, and after this time, TSB was discarded and samples were washed twice with DPBS to remove nonattached bacteria. After being washed, samples were treated in two different ways: to evaluate biomass production by the crystal violet assay (CV) and to evaluate bacterial growth by the microdilution assay.

In the CV assay, 100 μL of CV aqueous solution (1 mg/mL) was added to washed samples and incubated for 10 min at room temperature. After staining, samples were washed 3 times with DPBS. After removing DPBS, the biofilm was dissolved in 100 μL of acetic acid (30% v/v), and the absorbance was measured at 570 nm using a Varioskan LUX microplate reader (Thermo Fisher Scientific).

To evaluate bacterial growth, a microdilution assay was performed. 100 μL of DPBS was added to the washed samples, and then, they were sonicated for 1 min to release bacteria potentially embedded in the biofilms. Then, 1:10 serial dilutions of each sample were made in DPBS and 3 × 20 μL drops were seeded on TSA plates. Plates were incubated overnight at 37 °C, and bacteria colonies were counted in each drop. CFU/mL were calculated as follows:

$$\mathrm{CFU/mL} = \frac{\mathrm{number\ of\ colonies} \times \mathrm{dilution\ factor}}{0.02\ \mathrm{mL}} \quad (2)$$

2.8. Cell Cytotoxicity Evaluation *In Vitro*

The immortalized human keratinocyte cell line HaCaT was used, and the cytotoxicity was evaluated by the methyl tetrazolium (MTT) assay. Cells were seeded in 96-well plates at a density of 10,000 cells per well in 200 μL of DMEM High-Glucose media supplemented with 1% antibiotic and 10% FBS and incubated overnight. Then, the dried samples of RD, RR, Au@RD NPs, and Au@RR NPs were dissolved in DMEM medium without antibiotics (1% FBS) by sonication for 10 min and added to the cells. The concentrations were $5 \times 10^{-6} - 5$ mg/mL for RD and RR extracts, respectively, while they were $1 \times 10^{-5} - 1$ mg/mL for Au@RD NPs and Au@RR NPs. After 24 h of incubation, fresh DMEM medium was added after washing with DPBS. After overnight incubation at 37 °C, the medium was removed, cells were washed with DPBS, and then 200 μL of MTT solution (0.5 mg/mL, DMEM without FBS) was added to each well. After 3 h of incubation, the MTT solution was removed, and the purple crystals of formazan were dissolved in 100 μL of DMSO:methanol (1:1, v:v). The absorbance was measured at wavelengths of 565 nm with a reference at 750 nm using a Tecan Infinite200 plate reader. Untreated cellular samples were used as a control. The experiments were performed in triplicate.

2.9. Real-Time Quantitative PCR Analysis (RT-qPCR)

The HaCaT cells were seeded in 6-well plates at a density of 900,000 cells per well in DMEM High-Glucose media supplemented with 1% antibiotic and 10% FBS and incubated at 37 °C for 24h. The tested dried samples were dissolved in DMEM medium without antibiotics through 10 min of sonication and then applied to the cells. After 24 h of incubation, cells were washed twice using DPBS and detached from the plate by incubation with trypsin. Total RNA was isolated using the Universal RNA Purification Kit (EUR_X, cat. no. E3598) following the manufacturer's instructions. cDNA synthesis was performed from 100 ng of total RNA, using the TranScriba Kit, cat. no. 4000−20, A&A Biotechnology according to the manufacturer's instructions. The cDNA samples were diluted 50-fold in nuclease-free water (EURx, Poland) and stored at −20 °C before RT-qPCR reaction.

Gene expression analyses were performed on a cDNA template as previously described[24] using Rotor-Gene Q thermocycler (Qiagen, Germany). Each reaction was performed in duplicates. No-RT samples and nontemplate controls (NTC) were included in selected runs. Infection-induced changes in gene expression were determined by comparing the expression of the target gene to the reference gene (GAPDH) in control samples (untreated cells), using the Pfaffl method,[25] according to the following equation:

$$\mathrm{Ratio} = E^{C_t\mathrm{Reference}} \Big/ E^{C_t\mathrm{Target}} \quad (3)$$

where E is the amplification efficiency and C_t is the threshold cycle.

The analyzed genes and the sequences of their corresponding primers are listed in the Supporting Information (Section S3. *Real-time quantitative PCR*: Table S2). The RT-qPCR reaction conditions are summarized in the Supporting Information (Section S3. *Real-time quantitative PCR*: Table S3).

2.10. *In Vivo* Study Using Zebrafish Larvae

Adult zebrafish (*Danio rerio*) were maintained at 28 °C with a 14 h light/10 h dark cycle. The fish were fed twice daily, with either commercial zebrafish feed (Skretting, Norway) or live Artemia (Priroda Green, Ecuador). Zebrafish larvae were maintained in E3 medium supplemented with methylene blue (17.2 g/L NaCl (Chempur, Poland), 0.76 g/L KCl (POCH, Poland), 2.18 g/L $CaCl_2$ (EuroChem BGD, Poland), 2.4 g/L $MgSO_4$ (POCH, Poland), and 0.00005% (w/v) methylene blue (Sigma-Aldrich, Co., USA) at 28 °C. Studies were performed using wild-type AB × TL strain (cross-contamination of commonly used AB and TL wild-type zebrafish lines). Zebrafish husbandry was carried out at the Institute of Zoology and Biomedical Research, Jagiellonian University Zebrafish Core

https://doi.org/10.1021/acsbiomaterials.5c01488
ACS Biomater. Sci. Eng. 2026, 12, 1508−1521

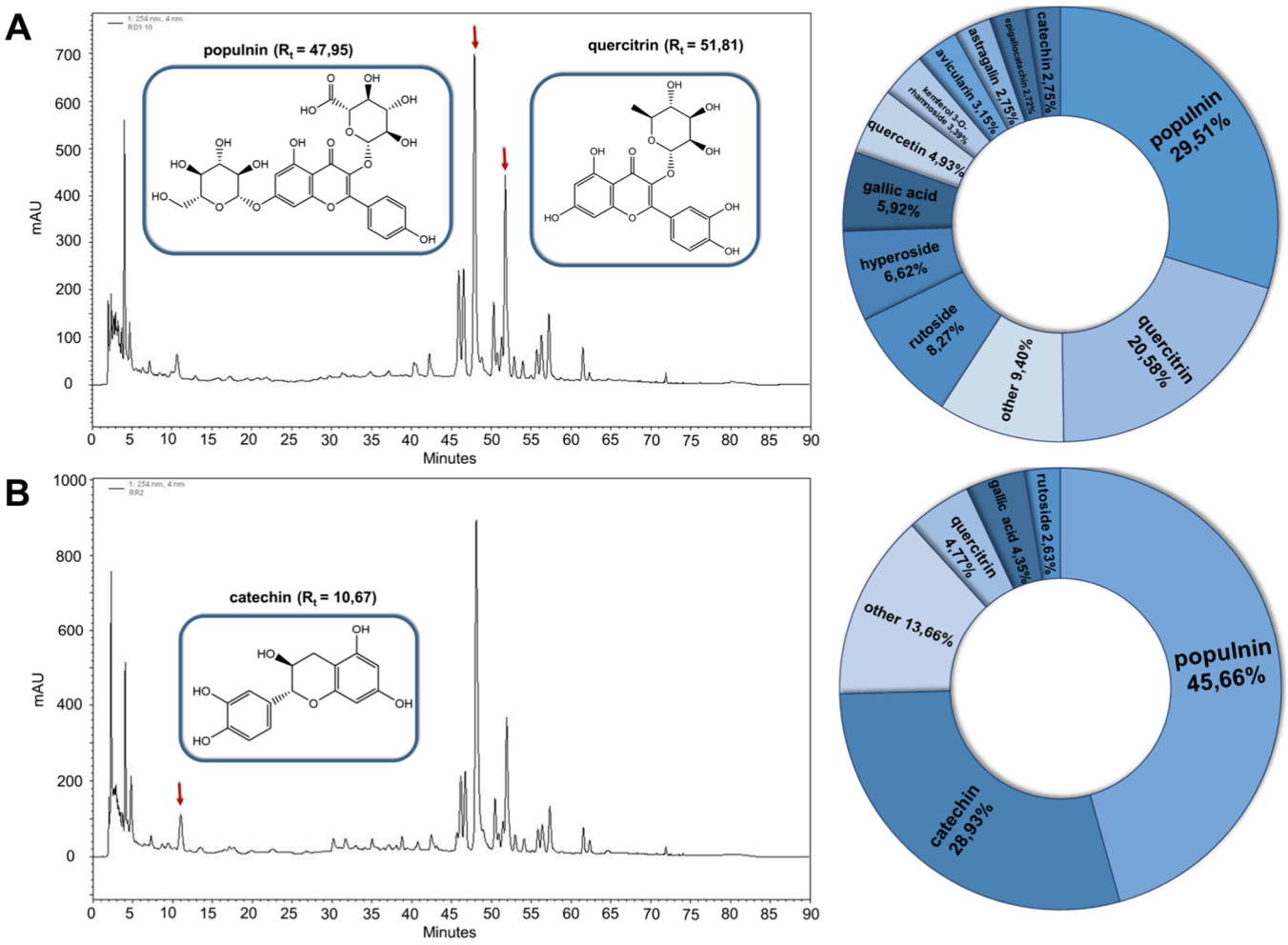

Figure 1. Percentage composition with representative examples of HPLC chromatograms obtained for each extract: (A) *Rosa damascena* extract (buds) and (B) *Rosa rugosa* extract (petals).

Facility, licensed under the District Veterinary Inspectorate in Krakow registry; Ministry of Science and Higher Education record no. 022 and 0057. All experiments were conducted in accordance with the European Community Council Directive 2010/63/EU. All methods involving zebrafish larvae followed ARRIVE guidelines.

Zebrafish larvae were treated with the tested extracts and/or colloids at 2 days postfertilization (2 dpf) either by immersion (addition of tested compounds to the E3 buffer) or by systemic microinjection onto the Duct of Cuvier as described previously.[26] Zebrafish were monitored daily for mortality and disease symptoms development. Studies on zebrafish larvae were performed up to 5 days postfertilization, which do not require approval from the local Ethics Committee. On day 5, all larvae participating in the experiment were euthanized in an overdosed MS-222 anesthetic according to standard procedure. At least 100 individuals were tested in each experimental group. The description of the investigated samples for *in vivo* tests is summarized in the Supporting Information along with the explanation of sample preparation (Section S4. *In vivo study on Zebrafish larvae*: Table S4).

2.11. Statistical Analysis

Each bar graph presents values in the form of mean ± standard deviation. One-way ANOVA followed by Tukey's test was applied in the case of cytotoxicity experiments *in vitro* and *in vivo*. Meanwhile, two-way ANOVA test was used to statistically analyze the data using Dunnett's post-test in the case of multiple comparations (antimicrobial assays). All statistical analyses were carried out using Prism 8 (GraphPad Software, San Diego, CA, USA). Experiments were conducted with three replicates, and all conditions were assessed in triplicate, unless indicated differently. Differences were considered statistically significant at $p \leq 0.05$. Other p values are indicated in the corresponding graphic.

3. RESULTS AND DISCUSSION

Facing the challenge of increasing the bioavailability of bioactive plant-derived compounds, the burgeoning development of nanotechnology and nanomaterials brings hopes to design and validate novel organic−inorganic hybrid nanomaterials.[27−30] The idea of the functionalization of nanoparticles (NPs) with bioactive phytochemicals originating from plant extracts (i.e., polyphenols, flavonoids, alkaloids, and other derivatives) nowadays attracts considerable interest due to their improved biocompatibility, stability, and multifunctional characteristics, in particular the undiscovered ones resulting from the additivity or synergy of a multicomponent system.[31−34]

3.1. Compositional Analysis of Rose Extracts

To explain which of the organic components derived from the rose extract plays a key role in the reduction of Au(III) ions and the stabilization of the resulting nanostructures, a qualitative and quantitative analysis of the investigated aqueous RD and RR extracts was performed by high-performance liquid chromatography (HPLC). Populnin (kaempferol 7-*O*-glucoside) was the dominant constituent in both extracts. Note-

https://doi.org/10.1021/acsbiomaterials.5c01488
ACS Biomater. Sci. Eng. 2026, 12, 1508−1521

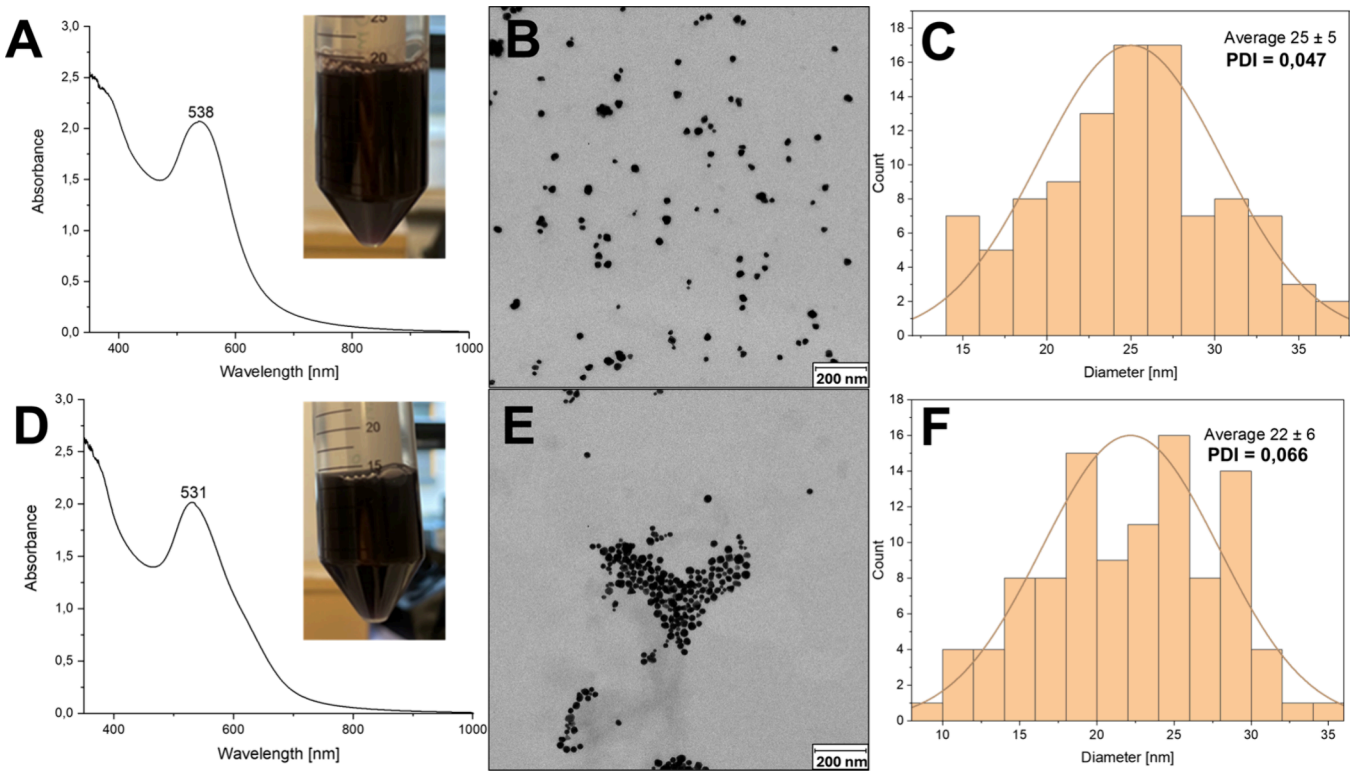

Figure 2. UV−vis spectra, TEM images, and size-distribution histograms for Au@RD NPs (A−C) and Au@RR NPs (D−F), respectively.

worthy, the percentage content of populnin in the RR extract was significantly higher than that in the RD extract (RD: 29.51%, RR: 45.66%). Populnin is a kaempferol, belonging to the flavonoids, attached via a glycosidic bond to β-D-glucopyranosyl groups at position 7. As a metabolite of many plants, it mainly functions as a free radical scavenger.[35] For the RD, quercitrin (quercetin 3-*O*-rhamnoside) was singled out as the second dominant constituent (RD: 20.58%, RR: 4.77%). Analyzing its chemical structure, it is a quercetin linked to the α-l-rhamnosyl group at position 3 via a glycosidic bond. It acts as an antioxidant, an inhibitor of many enzymes, and exerts a protective function against parasites.[36] The RR extract, in addition to populnin, contains significant amounts of catechin (RD: 2.75%, RR: 28.93%), which is a natural compound from the flavonoids group. It exhibits anti-inflammatory, antioxidant, and chemopreventive effects.[37] The pie charts presented in Figure 1 show the content of the predominant constituents in the individual extracts collected from RD and RR extracts prepared from buds and petals, respectively, with their corresponding chromatograms. Detailed HPLC analysis is presented in the Supporting Information along with the pie chart for RD extract from petals included for comparison purposes (Section S5. *Compositional analysis of rose extracts*: Table S5, Figure S1).

To find out if the composition varied in buds and petals for the same plant, a comparative HPLC analysis was carried out for extracts from buds (RD) and petals (RD, RR) of the same plant. This study revealed insignificant differences in the percentage composition of the most concentrated components, i.e., populnin (29.51%, 21.94%), quercitrin (20.58%, 18.38%), rutoside (8.27%, 9.60%), and hyperoside (6.62%, 7.97%) extracted under the same experimental conditions from the buds (RD) and petals (RD*) of *Rose damascena*, respectively. Such minor differences did not affect the quality and synthesis kinetics of the subsequent Au NPs syntheses (*vide infra*). Also, due to the previous studies on bud extracts,[23] it was decided herein to continue the research only with this type of extract.

3.2. Characteristics of Au NPs Obtained Using Rose Extracts

Plant-mediated synthesis of metallic nanostructures according to ecofriendly, efficient, and controlled protocols offers hybrid inorganic−organic nanostructures with potential and, most importantly, undiscovered activity, with even potential additive or synergetic activity. Our earlier scientific findings revealed that Au NPs synthesized with the aqueous extract of *Rosa damascena* (Au@RD NPs) exhibit selective cytotoxicity against cancer cells (HL60, A549) over peripheral blood mononuclear lymphocytes (PBML). Furthermore, a significantly higher level of DNA damage was demonstrated in cancer cells than in healthy somatic cells by the comet assay.[23] This encouraged us to continue the study of rose extracts to analyze also their antimicrobial potential. Natural antimicrobial activity of rose extracts is now widely investigated and well-documented in the latest literature,[38,39] drawing attention to the biocompatible potential of these extracts, which can replace synthesized chemical antiseptics and bactericidal.[40,41] Importantly, as well, an increasing number of scientific reports demonstrate clinical trials of the use of rose extracts, in various medical applications, for instance topical treatment,[42,43] wounds healing,[44] neuro-cognitive disorder and depression,[45] menopausal symptoms,[46] and food contact packing.[47,48] This emphasizes the application potential of the investigated hybrid materials containing rose extracts.

Plants and plant-derived extracts reduce metal ions, following a natural detoxification process. Such a sustainable approach combining two active components − metal NPs and plant-derived metabolites − might indicate a high therapeutic

https://doi.org/10.1021/acsbiomaterials.5c01488
ACS Biomater. Sci. Eng. 2026, 12, 1508−1521

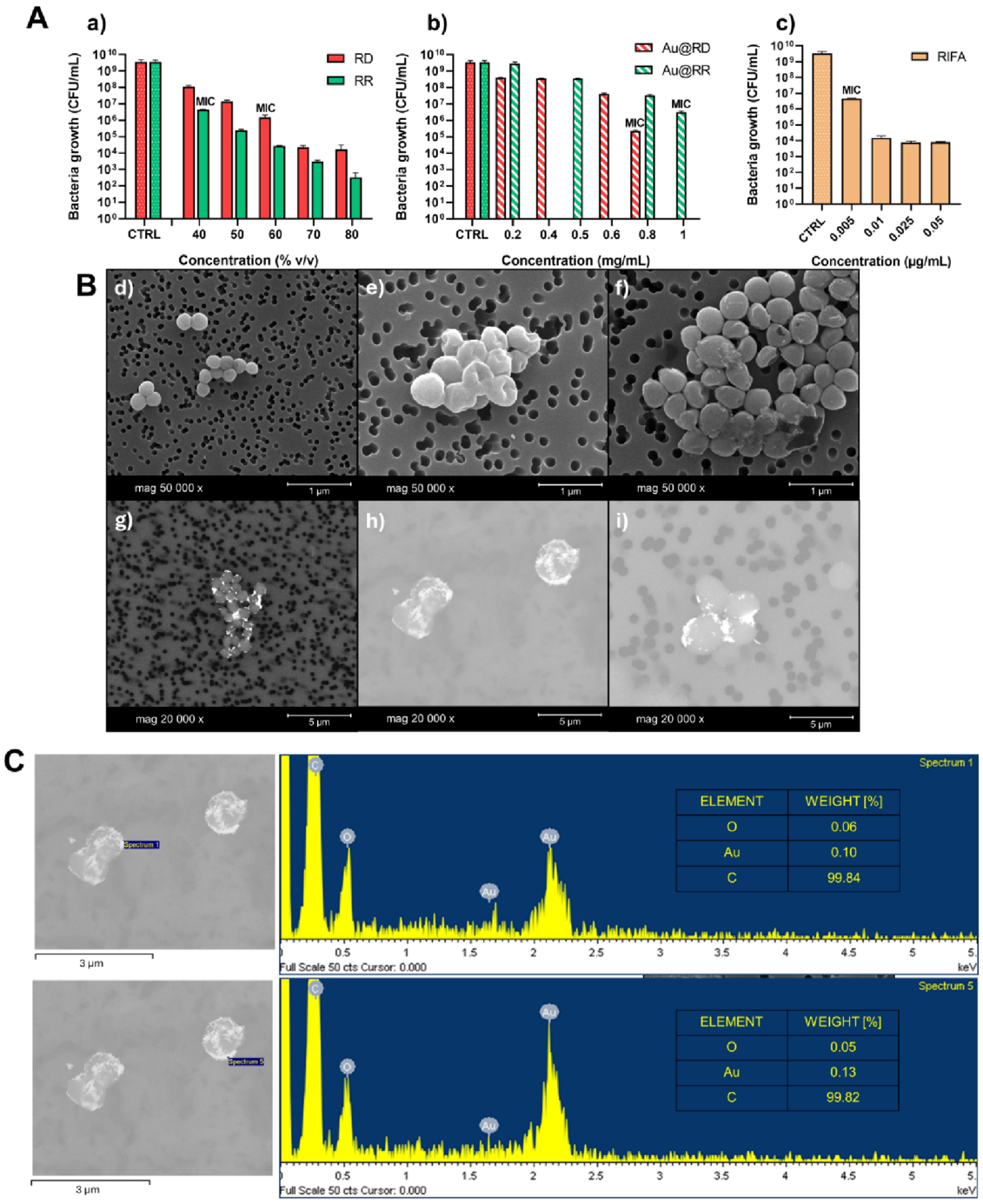

Figure 3. (A) Antimicrobial activity of (a) rose extracts (RD, RR), (b) gold nanoparticles (Au@RD NPs, Au@RR NPs), and (c) the antibiotic (rifampicin, RIFA in the figure legend). (B) Visualization of the antimicrobial activity of biologically active compounds by SEM for MRSA bacteria strain; (d) untreated control; treated bacteria with (e) RR extract 50% (v/v), (f) rifampicin 0.005 μg/mL, (g) Au@RR NPs 0.8 mg/mL, (h) Au@RR NPs 1 mg/mL, and (i) Au@RD NPs 0.6 mg/mL. Images (h) and (i) were taken using a backscattered electron (BSE) detector to highlight the sharp contrast between the metal NPs and the surrounding organic material. (C) EDX analysis report for a sample treated with Au@RR NPs at a concentration of 1 mg/mL.

potential of such hybrid NPs and allows us to discover their unknown additive/synergetic activities. In the synthesis of Au@RD NPs and Au@RR NPs colloids, the optimum time was established to be 2 h, leading to monodisperse colloids in terms of size and morphology. Most observed nanostructures are spherical or near-spherical in shape. No rod-type nanostructures, planar triangles, spikes, or other structures were noted in any of the TEM images analyzed. As confirmation of their monodisperse nature, narrow UV−vis spectra having reduced peak widths at half heights with a clear absorbance at 530−540 nm (Figure 2) were observed.

Monitoring the kinetics of the Au(III) ions reduction, significant changes in the rate of this process were observed. In the case of both extracts, stable and monodisperse colloids were obtained after 2 h of reaction. However, differences in the shape of the UV−vis spectrum (the appearance of a shoulder) and a hypochromic shift of SPR from 538 nm (Au@RD NPs) to 531 nm for Au@RR NPs were noticed (Supporting

https://doi.org/10.1021/acsbiomaterials.5c01488
ACS Biomater. Sci. Eng. 2026, 12, 1508−1521

Information: Figure S2, Section S6. *UV−vis monitoring of kinetics of AuNPs formation*). This indicates the formation of slightly smaller NPs for the latter, however, with a tendency to agglomerate as corroborated in Figure 2E. In-depth physicochemical characterization of the resulting colloids allowed us to determine the average physical/hydrodynamic diameters being 25 ± 5 nm (PDI = 0.05)/39 ± 0.3 nm (PDI = 0.3) for Au@RD NPs and 22 ± 6 nm (PDI = 0.07)/35 ± 0.7 nm (PDI = 0.5) for Au@RR NPs. Furthermore, zeta potential values were determined for the investigated colloids and were −35.83 ± 0.69 mV (pH = 3.84) and −32.37 ± 1.06 mV (pH = 3.74) for Au@RD NPs and Au@RR NPs, respectively. The latter results indicate good colloidal stability for the resulting dispersions. These results are also in agreement with the stability tests conducted in cellular media, which are necessary for the proper performance in the *in vitro* biological tests and for their potential assessment in medical applications. The conducted investigation did not show significant spectral changes in the UV−vis spectra during incubation in the DMEM medium supplemented with 1% FBS over 24 h at different temperatures (Supporting Information: Section S7. *Stability of gold nanoparticles (Au@RD and Au@RR NPs) in DMEM media)*: Figure S3).

Three compounds − populnin, catechin, and quercitrin, identified as the main components derived from RD and RR extracts (*vide supra*) − were selected to study their reducing and stabilizing activities on the ionic gold precursor. The synthesis of Au NPs with these compounds and their mixtures was carried out under comparable conditions to those when using the entire multicomponent extract. It was concluded that none of the compounds alone can reduce Au(III) ions and stabilize the resulting Au NPs. Colloids of comparable morphology, size, and polydispersity to the ones obtained from the whole extracts were obtained only in the case of a mixture of populnin and catechin or polpulnin and quercitrin of a similar composition (Supporting Information: Section S8. *Synthesis of Au NPs using polyphenols as reducing and stabilizing agents*: Figure S4). However, the stability of such dispersions was very poor (*vide* photos). The best results, most similar to the use of pure rose extracts, were obtained for multicomponent mixtures of populnin, catechin, quercitrin, and gallic acid, occurring at the highest concentrations tested. This confirmed the assumption that the multicomponent nature of real extracts is required to stabilize Au colloids under the conditions tested. At the same time, no single plant metabolite was indicated to play a significant role in the conducted syntheses of stable Au NPs. We hypothesized that the multicomponent mixture was needed for the reduction, capping, and stabilization of the resulting NPs because different chemical functions are required to carry out those three effects, and no single molecule can provide them simultaneously. In addition, the synergistic interactions among the multicomponent mixture create a mild yet efficient redox environment, with its corresponding dynamic stabilization effect. To corroborate these findings and in agreement with our other investigations on polysaccharides (i.e., chitosan) and their reductive potential toward Ag(I) and Au(III) ions,[49,50] we demonstrated that small phenolic compounds such as quercetin and quercitrin (a glycoside form that originated from quercetin and the deoxy sugar rhamnose) in a mixture are more potent reducing/stabilizing agents as chitosan alone is in the reduction of Au(III) ions (Supporting Information: Section S8. *Synthesis of Au NPs using polyphenols as reducing and stabilizing agents*: Figure S5).

3.3. Determination of Minimum Inhibitory Concentration Values

MIC values for (i) aqueous extracts of RD and RR, (ii) the colloids Au@RD NPs and Au@RR NPs, and (iii) the antibiotic rifampicin were determined *in vitro* against methicillin-resistant *Staphylococcus aureus* (MRSA). The dependence of the number of MRSA colonies on the concentration of the tested extract/colloid/antibiotic, together with the indicated MIC values, is presented in Figure 3A.

The MIC value was determined as the value corresponding to the minimum concentration of the extract, colloid, and antibiotic, causing a decrease in the number of bacterial colonies of more than two logs compared to untreated controls. In the case of RD extracts, the MIC was 60% (v/v), while that for the RR was 40% (v/v). These differences can be explained by the different compositions of the extracted compounds, as determined using the HPLC technique. The determined concentrations of the individual compounds were markedly different, which influenced the observed activity of the tested extracts, both in terms of the reduction potential of the extract against Au(III) ions and on the observed biological effect *in vitro*. In the case of the semisynthetic antibiotic rifampicin, the MIC value was reached as very low concentrations (*i.e.*, 0.005 μg/mL) as expected for this potent ansamycin antibiotic. MIC values of 0.8 and 1 mg/mL were determined for Au@RD NPs and Au@RR NPs, respectively. The lower MIC for Au@RD NPs compared to that for Au@RR NPs can be explained by its higher gold content in the resulting colloid, as it was determined by inductively coupled plasma−mass spectrometry (ICP-MS) (Au@RD NPs: 0.092 ± 0.001 mg Au/mg NPs; Au@RR NPs: 0.061 ± 0.002 mg Au/mg NPs).

Scanning electron microscopy (SEM) allowed us to visualize the effect of the tested compounds on the tested MRSA bacterial strain (Figure 3B). In detail, Figure 3B(d) shows the characteristic spherical morphology of untreated bacteria. The image of bacteria treated with a 50% (v/v) solution of RR extract (Figure 3B(e)), a concentration 10% higher than the MIC value observed, showed that the cell wall was compromised, having large depressions/concavities, which may indicate damage to this structure. In contrast, Figure 3B(f)) shows that the antibiotic rifampicin at a concentration equal to its measured MIC value (0.005 μg/mL) did not induce important membrane damage attributed to its reported intracellular mechanism of antimicrobial action (i.e., by inhibiting DNA transcription by binding to the bacterial RNA polymerase enzyme). In the case of RR extracts, further studies are needed to precisely determine the biological targets in the bacterial cell that might be responsible for their antimicrobial action. The images in Figure 3B(g)−(i) show a visualization of the bacterial effect of Au@RR NPs (0.8 mg/mL), Au@RR NPs (1 mg/mL), and Au@RD NPs (0.6 mg/mL), respectively. By backscattered electron detection (BSED), we observed interaction of the Au NPs with the surface of the bacterial cells, probably due to supramolecular interactions (e.g., hydrogen bonding). This could suggest that their mechanism of action is to degrade or disrupt the integrity of the bacterial wall.

In addition, energy-dispersive X-ray spectroscopy (EDX) analysis was performed on selected samples to confirm the

https://doi.org/10.1021/acsbiomaterials.5c01488
ACS Biomater. Sci. Eng. 2026, 12, 1508−1521

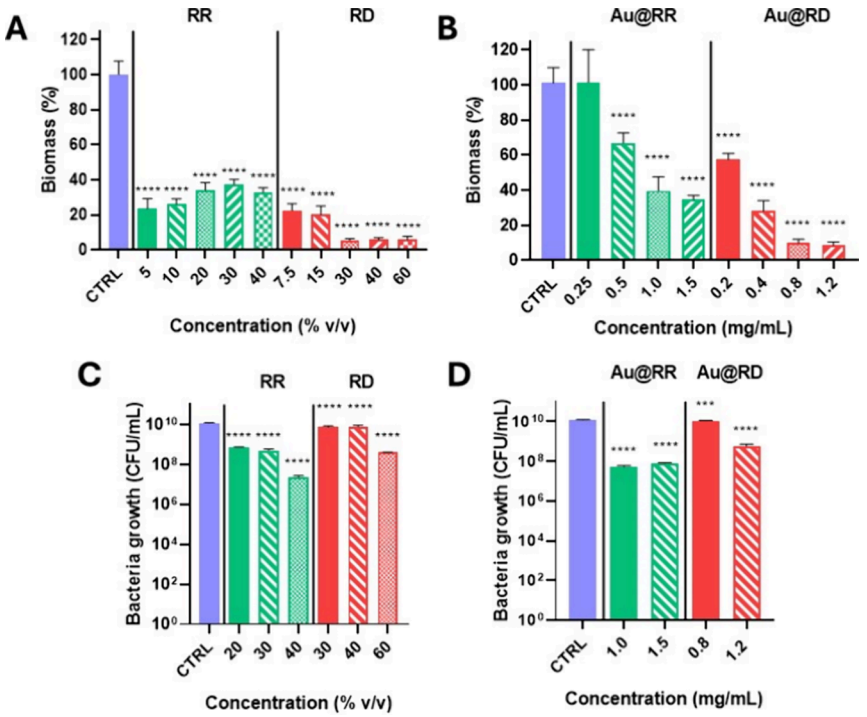

Figure 4. MRSA biofilm inhibition: (A, B) reduction of biomass production determined by the CV assay; (C, D) inhibition of bacteria growth evaluated by the microdilution assay. Statistically significant differences between sample and growth control are indicated as **** $p < 0.0001$ and *** $p < 0.001$.

presence of gold. Gold was detected, as well as organic matter attributed to the presence of organic material derived from polyphenols, flavonoids, and other organic compounds contained in the rose extracts. Figure 3C shows a representative example taken at two different points in a bacterial sample treated with Au@RR NPs with a concentration equal to its MIC value (1 mg/mL).

3.4. Determination of Fractional Inhibitory Concentration Index

We also investigated the possibility of potential additive or synergy effects between rose extracts and antibiotics to potentially reduce the doses of antibiotics required to exert antimicrobial action and, consequently, to reduce the chances to develop resistance. Conjugates of metallic NPs with antibiotics, or other substances with reported antimicrobial activity, have many advantages such as improved efficacy against several targets, having multiple mechanisms of action, slowing the emergence of resistant microorganisms, reducing required doses to exert an effect, or increasing the spectrum of antimicrobial activity[33]

To determine a possible type of interaction (additive/synergistic) between the selected antibiotic and the studied RR plant extracts, the FICI value was determined as depicted in the Supporting Information (Section S9. *Fractional inhibitory concentration index (FICI)*: Figure S6). It was shown that additivity (FICI = 0.626 ± 0.160) was observed for combinations of RR extracts and selected antibiotic. This type of interaction indicates different mechanisms of antimicrobial action for both compounds, resulting in an additive antimicrobial effect when combined. Although no synergy was observed, an additive effect might be beneficial when treating pathogenic bacteria because lower doses for the individual antibiotic would be needed in combination with RR plant extract while still achieving the desired therapeutic effect and, consequently, reducing the chances of developing resistance. In our study, we addressed AMR through two complementary strategies. On the one hand, the use of rose-derived extracts enables a reduction in the required antibiotic concentration to achieve effective antimicrobial activity. On the other hand, both the broad-spectrum phytochemical antimicrobial effect of the plant-derived extracts and the multifunctional antimicrobial mechanisms of their corresponding Au NPs contribute to minimizing the likelihood of resistance development.

3.5. Study on Antibiofilm Activity *In Vitro*

Biofilm inhibition experiments were performed by using the crystal violet (CV) assay and the microdilution method (Figure 4) to elucidate the effectiveness of the developed colloids against sessile bacteria.

Considering the CV results for both extracts (RD, RR), a large inhibition in the production of the biomass was observed at all tested concentrations. For Au NPs colloids, a decrease in the formed biomass was also measured, except for Au@RR NPs at the lowest concentration tested. For both extracts and nanoparticles obtained from RD, greater inhibitory activity was observed in terms of biomass reduction relative to that measured for the compounds containing RR. To determine whether the inhibition of biofilm formation was attributed to a lack of viable bacteria or to a reduction in biomass production, the microdilution test was carried out, concluding that biomass production was inhibited and a slight antimicrobial effect was observed at the highest doses tested. It should also be taken into account that some components present in the tested compounds could inhibit the communication pathways in bacteria (quorum sensing, QS) as reported for other plant-derived extracts.[51,52] The differences in the observed inhibitory activities for the RD and RR-containing compounds could be attributed to their different compositions. The RD extract from

https://doi.org/10.1021/acsbiomaterials.5c01488
ACS Biomater. Sci. Eng. 2026, 12, 1508−1521

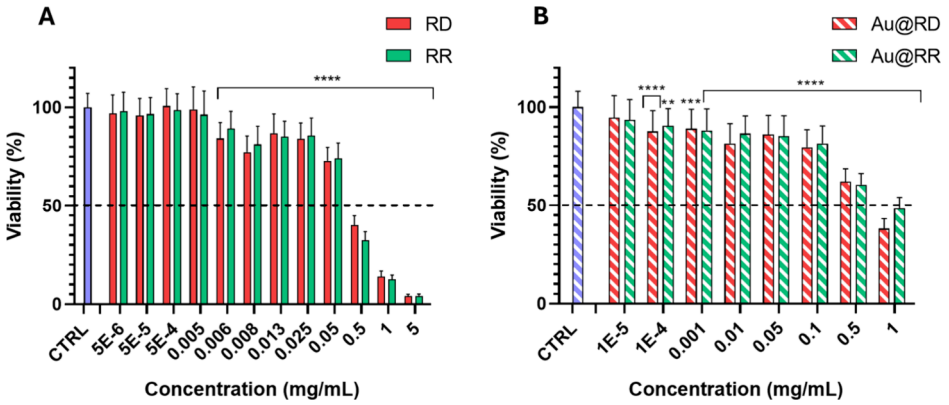

Figure 5. Concentration-dependent viability of HaCaT cells 24 h after incubation with RD and RR extracts (A) and Au@RD NPs and Au@RR NPs (B). All the experiments were performed at least three times in triplicate. ****, ***, **Statistically significant differences between sample and growth control: $p < 0.0001$, $p < 0.001$, $p < 0.01$, respectively.

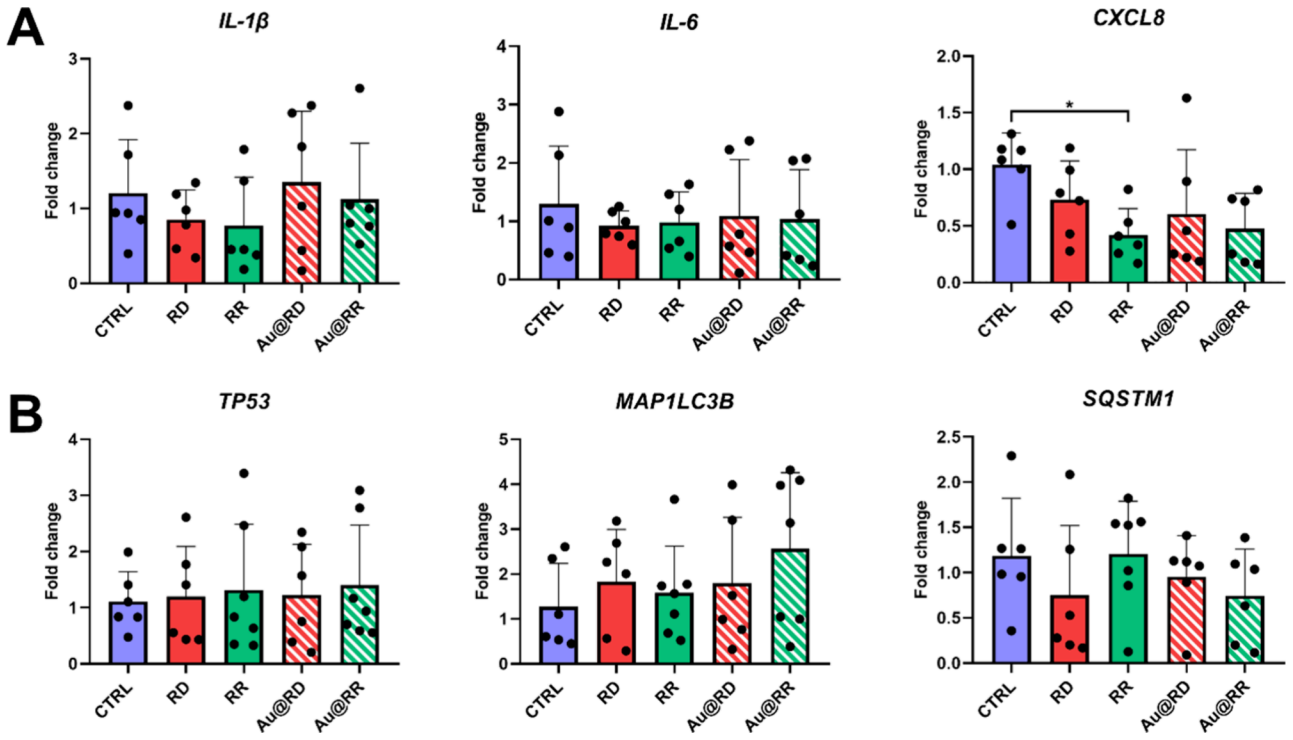

Figure 6. Effect of tested compounds at selected concentrations on the gene expression of the pro-inflammatory cytokines (A) and apoptotic/autophagic markers (B) and in HaCaT cells after 24 h of treatment. CTRL − control (untreated cells), RD − 0.05 mg/mL RD extract, RR − 0.05 mg/mL RR extract, Au@RD − 0.1 mg/mL Au@RD NPs, Au@RR − 0.1 mg/mL Au@RR NPs. The *GAPDH* gene was used as a reference. All of the experiments were performed at least 6 times. Each dotted line represents one sample. Data are presented as means + SD. Statistical significance (in comparison to the control group) was analyzed using one-way ANOVA followed by Tukey's test. *Statistically significant difference between RR sample and control ($p \leq 0.05$).

buds contained a significantly larger amount of quercitrin, a derivative of quercetin, which, according to the literature, has a bacteriostatic and antibacterial effect[53−55]

3.6. Cytotoxicity Studies *In Vitro*

To assess the safety of the tested biologically active compounds *in vitro*, the immortalized human keratinocyte line HaCaT was used, and the cells were treated with different concentrations of rose extracts and gold nanoparticle colloids. The cytotoxic effect of the compounds was evaluated using the MTT assay 24 h after treatment (Figure 5).

The results indicate the comparable effect of both RR and RD extracts on HaCaT cell viability. RR and RD extracts at the concentration of 0.05 mg/mL or lower did not induce significant cytotoxicity (viability: for RD 73 ± 7%, for RR 74 ± 8%). Rose extracts combined with gold nanoparticles exhibited even lower toxicity than the extracts themselves. At a comparable concentration of 0.05 mg/mL, these compounds were not cytotoxic to the cells (viability for Au@RD: 86 ± 10%; for Au@RR: 85 ± 10%); however, at a higher concentration of 0.5 mg/mL, the treatment resulted in decreased cell viability (Au@RD: 62 ± 7%; Au@RR: 61 ± 6%). Noteworthy, for concentrations equal to the MIC values that were 0.8 and 1 mg/mL for Au@RD NPs and Au@RR NPs, respectively, around 50% of cells were viable. This observed dose-dependent cytocompatibility allows one to

https://doi.org/10.1021/acsbiomaterials.5c01488
ACS Biomater. Sci. Eng. 2026, 12, 1508−1521

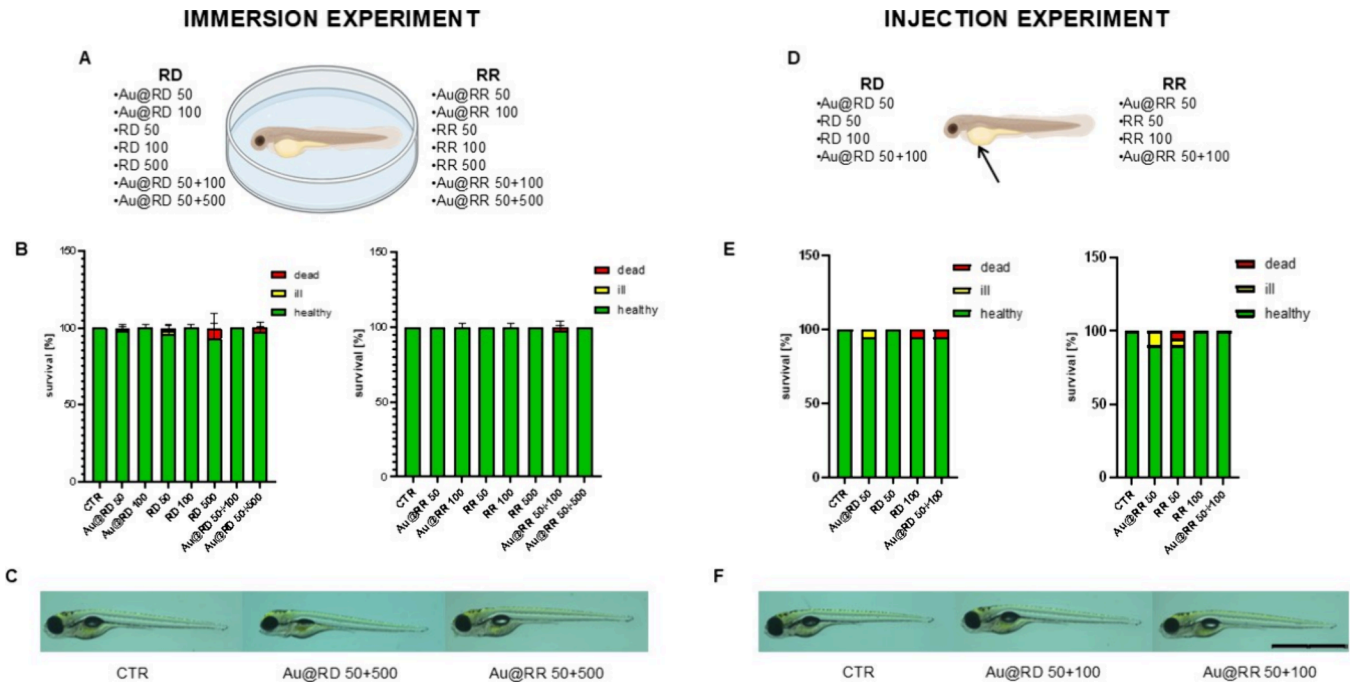

Figure 7. Assessment of the toxicity of the tested compounds using zebrafish larvae. Larvae were treated with selected compounds at indicated concentrations by either immersion (A−C) or systemic microinjection (D−F). (A, D) Experimental schemes, (B, E) percentage of healthy, ill, or dead larvae 72 h after treatment with the compounds. (C, F) representative images of zebrafish larvae 72 h after treatment with the compounds. All concentrations of tested compounds are in μg/mL; "+" indicates a mixture of nanoparticles and appropriate extract. Statistical significance (in comparison to the control group) was analyzed using one-way ANOVA followed by Tukey's test. Data did not reveal statistically significant differences. $N = 50$. The scale bar is 1 mm.

assume that the investigated nanocolloids, in appropriately selected doses, can be used as safe, biocompatible, bacteriostatic materials.

The above results are in line with the reports of Wang et al.,[56] showing a low cytotoxic effect of Au NPs enriched with RR extract, *in vitro*, and also on HaCaT cells. Furthermore, our findings are in agreement with other authors who claim that spherical NPs obtained using the plant extract (physical size up to ca. 30 nm) are less toxic than their anisotropy counterparts.[57] In general, it can be postulated that the plant extracts, as a source of reducing and stabilizing agents, lead to the formation of Au NPs coated with nontoxic biological molecules. Such nanoformulations contribute to lower cytotoxic effects compared to chemically synthesized Au NPs.

3.7. *In Vitro* Analysis of Gene Expression upon Treatment by Reverse Transcription Quantitative PCR (RT-qPCR)

To further confirm the safety of rose extracts and the corresponding Au nanocolloids, the regulation of gene expression for inflammatory and cell death markers were investigated. HaCaT cells were treated with the investigated extracts and colloids, and the gene expression was evaluated after 24 h of treatment compared with the untreated control cells.

Importantly, none of the tested compounds induced the significant expression of pro-inflammatory cytokines genes *IL-1β*, *IL-6*, and *CXCL8* in HaCaT cells (Figure 6A). Interestingly, in the group treated with the *Rosa rugosa* extract (RR), a significant downregulation of the *CXCL8* gene was observed compared to that of the control. *IL-8* is a key pro-inflammatory chemokine involved in neutrophil recruitment and the amplification of inflammatory responses. The absence of *CXCL8* induction, together with unchanged levels of *IL-1β* and *IL-6*, indicates that these systems do not exert broad immunosuppressive effects but rather maintain a noninflammatory state, which is advantageous for therapeutic strategies.

Next, the expression of genes involved in cell death particularly related to apoptosis and autophagy − *TP53* (gene encoding tumor protein 53), *MAP1LC3B* (gene encoding ubiquitin-like microtubule-associated protein 1 light chain 3 beta), *SQSTM1* (gene encoding sequestosome protein 1/SQSTM1) − were evaluated. Results showed the expression of the *TP53* gene at control levels in all experimental conditions (Figure 6B), indicating an antiapoptotic effect. The *TP53* gene encodes p53 protein, which is responsible for activating DNA repair mechanisms or directing damaged cells toward apoptosis.[58] Upregulation of this gene is often observed for compounds with anticancer/pro-apoptotic profiles.[59]

In general, nanomaterials can lead to autophagy, a process of cell death regulation by recycling proteins and organelles from damaged cells. This is realized by transporting inessential or harmful materials (i.e., nanomaterials) to lysosomes for degradation and recycling. The final and obligatory steps for the termination of autophagy are the fusion of autophagosomes and lysosomes and the formation of autolysosomes.[60,61] Hence, next, the impact of tested compounds on the expression of autophagic markers, representing control points at different stages of the process induction, was evaluated. *MAP1LC3B* that encodes the LC3 protein is responsible for the cellular autophagic flux and is essential for autophagosome formation. While *SQSTM1* is a key indicator of lysosomal degradation as it binds various misfolded protein aggregates and recruits them to autophagosomes for clearance.[62] Analysis of gene expression showed that none of the tested formulations (extracts alone and the corresponding Au nanocolloids) significantly increased the expression of both autophagy

https://doi.org/10.1021/acsbiomaterials.5c01488
ACS Biomater. Sci. Eng. 2026, 12, 1508−1521

markers *MAP1LC3B* and *SQSTM1* (Figure 6B). These results are in agreement with the latest work revealing that the Au NPs induce autophagosome accumulation resulting from blockade of autophagy flux and leading to lysosomes impairment, rather than induction of autophagy.[63,64]

Overall, these results indicate that the rose extracts (RD and RR) and Au nanoparticles (Au@RD NPs and Au@RR NPs) at tested concentrations do not induce inflammatory response and apoptotic/autophagic cell death of HaCaT cells, supporting our previous observations of cell viability. These compounds can be considered biocompatible, potentially reach therapeutic concentrations, and be further tested *in vivo*.

3.8. *In Vivo* Study Using Zebrafish Larvae

Currently, due to the rapid development of nanosystems for drug discovery, *in vivo* models are needed to perform a wide-scale screening of these formulations. However, rodent models are expensive, time-consuming, and ethically restricted, which limits the number of potential drugs feasibly assessed in a single study. In contrast, zebrafish (*Danio rerio*) is a very powerful model for high-throughput drug screening, and it is widely used for toxicological studies.[65] Moreover, zebrafish share high genetic and anatomical similarities with humans[66] and conserved cellular mechanisms, allowing for successful testing of potential drugs for human diseases and uncovering their mechanism of action.[67] In addition, larval transparency allows for easy observation of any unwanted side effects of the tested compound. It is also possible to conduct studies on many zebrafish larvae in experimental groups, thus allowing for the drawing of statistically significant conclusions. Therefore, next, an *in vivo* zebrafish larval model was employed to assess the toxicity of the tested compounds (Figure 7). A detailed description of experimental conditions along with the explanation of sample preparation is included in the Supporting Information (Section S4. *In vivo study using zebrafish larvae*: Table S4).

To evaluate the toxicity of the tested compounds, the two most commonly used approaches were utilized − the immersion and intravenous microinjection methods.[68] During immersion, tested compounds were directly added to the fish tank medium, allowing for absorption through the skin and gills. As the final concentration absorbed by the fish is unknown in this experimental case, furthermore, precise investigations are needed. However, these results show the lack of toxic effects (Figure 7A−C) when the animals were exposed to external contact with the nanomaterials and to their absorption from the environment in which they live. Then, microinjection was performed intravenously into the Duct of Cuvier, ensuring a systemic distribution of the tested compounds. At 72 h post-treatment, the number of healthy, ill (presenting any morphological abnormalities), or dead larvae was counted (Figure 7D−F). The results indicate that rose extracts and gold nanoparticles are nontoxic to zebrafish larvae even at the highest tested concentrations when applied by both immersion and microinjection. No significant changes in the larval death rate and morphology were observed in treated larvae, suggesting the biocompatibility of the investigated extracts (RD and RR) and the corresponding Au NPs (Au@RD NPs and Au@RR NPs). These observations are in line with the current results in general confirming nontoxicity of Au NPs on zebrafish embryos.[69−73]

To the best of our knowledge, this is the first time that the zebrafish model was used to test the rose extracts and Au NPs modified with rose extracts as biomimetic metallic nanoparticles. Overall, the *in vitro* and *in vivo* safety profile of the tested compounds supports their potential for further evaluation as antibacterial and immunomodulatory candidates while acknowledging that additional studies are necessary to confirm these properties. As zebrafish have been previously established for modeling human bacterial infections such as *Staphylococcus aureus*[74] or *Porphyromonas gingivalis*,[26] it can be a powerful tool to further study the effect of the compounds used in this study on infection with selected human bacterial pathogens.

4. CONCLUSIONS

In this study, biomimetic Au@RD NPs and Au@RR NPs obtained via a sustainable approach without any additional toxic reducing or stabilizing chemical reagents were synthesized and characterized. Only whole aqueous extracts of *Rosa damascene* and *Rosa rugosa* resulted in the formation of stable, monodisperse nanoparticles from metallic gold precursors, while individual compounds extracted from the roses were not enough to act as reducing and capping agents to produce stable metallic gold. Then, the biological study, both *in vitro* and *in vivo* in terms of cytotoxicity and antibacterial activity, revealed no acute cytotoxicity (HaCaT cell line, zebrafish larval model) but bacteriostatic activity at equivalent doses with potent inhibition of biofilm formation (MRSA strain). Noteworthy, the additivity of rose extracts with rifampicin improved the antibacterial activity of the individual components, indicating their different mechanism of antimicrobial action (observed also by SEM analysis) and highlighting the potential to combat the acquisition of bacterial resistance when combined. The absence of changes in the expression of pro-inflammatory cytokine genes such as *IL-1β* and *IL-6* or even decreasing the expression of *CXCL8* following treatment of HaCaT cells with rose extracts and the corresponding Au nanocolloids indicates that these compounds do not trigger an inflammatory response, suggesting their biocompatibility with human cells. Furthermore, evaluation of *TP53*, *MAP1LC3B*, and *SQSTM1* gene expression allowed us to suggest that neither apoptotic nor autophagic cell death as the dominating mode of action of the extracts and the resulting Au colloids on keratinocytes, in addition confirming their biosafety *in vitro*. In final, at the studied doses, the survival of *Danio rerio* larvae and their proper development (lack of deformities) confirmed biocompatibility *in vivo*.

Given these advantages, we envision a huge biomedical potential for Au@RD NPs and Au@RR NPs characterized by their colloidal stability, biocompatibility, and antibacterial potential against planktonic and sessile bacteria. These attractive inorganic−organic antibiotic-like hybrids composed of metal nanoparticles and plant-derived metabolites deserve further investigation as suitable alternatives to commercially available antibiotics. We anticipate that a combination therapy based on the proposed "metallo-drugs" will be a powerful way to combat antimicrobial resistance due to its multitargeted mode of action while being nontoxic systemically.

■ ASSOCIATED CONTENT

Data Availability Statement

Data will be made available on request. The data supporting this article have been included as part of the ESI† and will also

https://doi.org/10.1021/acsbiomaterials.5c01488
ACS Biomater. Sci. Eng. 2026, 12, 1508−1521

be available in the Cracow Open Research Data Repository (https://www.uj.rodbuk.pl/).

Supporting Information

The Supporting Information is available free of charge at https://pubs.acs.org/doi/10.1021/acsbiomaterials.5c01488.

List of analytical standards for HPLC quantification; Determination of minimum inhibitory concentration values; Real-time quantitative PCR; *In vivo* study using zebrafish larvae; Compositional analysis of rose extracts; UV−vis monitoring of AuNPs formation kinetics; Stability of gold nanoparticles (Au@RD and Au@RR NPs) in DMEM media; Synthesis of Au NPs using polyphenols as reducing and stabilizing agents; Fractional inhibitory concentration index (FICI) (PDF)

AUTHOR INFORMATION

Corresponding Author

Agnieszka Kyzioł − *Department of Inorganic Chemistry, Faculty of Chemistry, Jagiellonian University, Kraków 30-387, Poland;* orcid.org/0000-0002-5563-4508; Email: kyziol@chemia.uj.edu.pl

Authors

Julia Kulczyńska − *Department of Inorganic Chemistry, Faculty of Chemistry, Jagiellonian University, Kraków 30-387, Poland; Doctoral School of Exact and Natural Sciences, Jagiellonian University, Kraków 30-348, Poland*

Natalia Topa − *Doctoral School of Exact and Natural Sciences, Jagiellonian University, Kraków 30-348, Poland; Department of Evolutionary Immunology, Faculty of Biology, Jagiellonian University, Kraków 30-387, Poland*

Magdalena Widziołek − *Department of Evolutionary Immunology, Faculty of Biology, Jagiellonian University, Kraków 30-387, Poland*

Joanna Homa − *Department of Evolutionary Immunology, Faculty of Biology, Jagiellonian University, Kraków 30-387, Poland*

Inga Kwiecień − *Department of Medicinal Plant and Mushroom Biotechnology, Faculty of Pharmacy, Jagiellonian University, Kraków 30-688, Poland*

Enrique Gamez − *Instituto de Nanociencia y Materiales de Aragón (INMA), CSIC-Universidad de Zaragoza, Zaragoza 50009, Spain; Department of Chemical and Environmental Engineering, University of Zaragoza, Zaragoza 50018, Spain*

Manuel Arruebo − *Instituto de Nanociencia y Materiales de Aragón (INMA), CSIC-Universidad de Zaragoza, Zaragoza 50009, Spain; Department of Chemical and Environmental Engineering, University of Zaragoza, Zaragoza 50018, Spain;* orcid.org/0000-0003-3165-0156

Complete contact information is available at: https://pubs.acs.org/10.1021/acsbiomaterials.5c01488

Author Contributions

J.K.: Investigation, Data curation, Writing − Original Draft, Review & Editing. N.T.: Investigation, Data curation, Writing − Review & Editing. M.W.: Investigation, Writing − Review & Editing. J.H.: Methodology, Writing − Review & Editing. E.G.: Investigation (biofilm analysis), Writing − Review & Editing. I.K.: Investigation (HPLC analysis), Writing − Review & Editing. M.A.: Methodology, Writing − Review & Editing. A.K.: Methodology, Investigation, Data curation, Funding acquisition, Writing − Original Draft, Review & Editing, Supervision.

Notes

The authors declare no competing financial interest.

ACKNOWLEDGMENTS

This research was funded by the National Science Center of Poland (NCN) within the framework of the project OPUS 22 (2021/43/B/ST4/02833) given to Agnieszka Kyzioł. We acknowledge Olga Barczyk-Woźnicka (Institute of Zoology and Biomedical Research, Faculty of Biology, Jagiellonian University) for the transmission electron microscopy characterization of Au nanoparticles. Magdalena Widziołek thanks to NCN for the Sonata-18 project (2022/47/D/NZ6/02891). Manuel Arruebo acknowledges the Spanish Ministry of Science and Innovation (PID2023-146091OB-I00) for funding, and for the Severo Ochoa Programme for Centers of Excellence in R&D (CEX2023-001286-S MICIU/AEI/10.13039/501100011033).

REFERENCES

(1) Sengupta, S.; Chattopadhyay, M. K.; Grossart, H.-P. The multifaceted roles of antibiotics and antibiotic resistance in nature. *Front Microbiol* **2013**, *4*, 47.

(2) Costa, D. L. Health and the Economy in the United States from 1750 to the Present. *J. Econ Lit* **2015**, *53* (3), 503−570.

(3) Spellberg, B.; Gilbert, D. N. The Future of Antibiotics and Resistance: A Tribute to a Career of Leadership by John Bartlett. *Clinical Infectious Diseases* **2014**, *59* (suppl 2), S71−S75.

(4) Angelini, P. Plant-Derived Antimicrobials and Their Crucial Role in Combating Antimicrobial Resistance. *Antibiotics* **2024**, *13* (8), 746.

(5) Arip, M.; et al. Review on Plant-Based Management in Combating Antimicrobial Resistance - Mechanistic Perspective. *Front Pharmacol* **2022**, *13*, No. 879495.

(6) Akram, M.; Riaz, M.; Munir, N.; Akhter, N.; Zafar, S.; Jabeen, F.; Ali Shariati, M.; Akhtar, N.; Riaz, Z.; Altaf, S. H.; Daniyal, M.; Zahid, R.; Said Khan, F.; et al. Chemical constituents, experimental and clinical pharmacology of *Rosa damascena*: a literature review. *J. Pharm. Pharmacol.* **2020**, *72* (2), 161−174.

(7) Chen, Z.; Hong, N.; Xu, N.; Yan, C.; Cao, P.; Yao, H. In vitro efficacy of Rosa damascena solid state fermentation liquid and water extract on skin care. *Skin Research and Technology* **2024**, *30* (8), No. e13869.

(8) Mahboubi, M. Rosa damascena as holy ancient herb with novel applications. *J. Tradit Complement Med.* **2016**, *6* (1), 10−16.

(9) Rasooli, T.; Nasiri, M.; Kargarzadeh Aliabadi, Z.; Rajabi, M. R.; Feizi, S.; Torkaman, M.; Keyvanloo Shahrestanaki, S.; Mohsenikhah, M.; Rezaei, M.; Abbasi, M.; et al. *Rosa Damascena mill* for treating adults' anxiety, depression, and stress: A systematic review and dose−response meta-analysis of randomized controlled trials. *Phytotherapy Research* **2021**, *35* (12), 6585−6606.

(10) Xie, J.; Li, M.-X.; Du, Z.-Z. Chemical compounds, anti-aging and antibacterial properties of Rosa rugosa Purple branch. *Ind. Crops Prod* **2022**, *181*, No. 114814.

(11) Tursun, X.; et al. Anti-Inflammatory Effect of Rosa rugosa Flower Extract in Lipopolysaccharide-Stimulated RAW264.7 Macrophages. *Biomol Ther (Seoul)* **2016**, *24* (2), 184−90.

(12) Zhao, X.; Tang, H.; Jiang, X. Deploying Gold Nanomaterials in Combating Multi-Drug-Resistant Bacteria. *ACS Nano* **2022**, *16* (7), 10066−10087.

(13) Wang, C.; Wei, X.; Zhong, L.; Chan, C. L.; Li, H.; Sun, H. Metal-Based Approaches for the Fight against Antimicrobial Resistance: Mechanisms, Opportunities, and Challenges. *J. Am. Chem. Soc.* **2025**, *147* (15), 12361−12380.

(14) Świętek, M.; Ma, Y.-H.; Wu, N.-P.; Paruzel, A.; Tokarz, W.; Horák, D. Tannic Acid Coating Augments Glioblastoma Cellular

Uptake of Magnetic Nanoparticles with Antioxidant Effects. *Nanomaterials (Basel)* **2022**, *12* (8), 1310.
(15) Alfke, J.; Esselen, M. Cellular Uptake of Epigallocatechin Gallate in Comparison to Its Major Oxidation Products and Their Antioxidant Capacity In Vitro. *Antioxidants (Basel)* **2022**, *11* (9), 1746.
(16) Wang, H.; Wang, C.; Zou, Y.; Hu, J.; Li, Y.; Cheng, Y. Natural polyphenols in drug delivery systems: Current status and future challenges. *Giant* **2020**, *3*, No. 100022.
(17) Lamba, H.; Sathish, K.; Sabikhi, L. Double Emulsions: Emerging Delivery System for Plant Bioactives. *Food Bioproc Tech* **2015**, *8* (4), 709−728.
(18) Roy, A.; Bulut, O.; Some, S.; Mandal, A. K.; Yilmaz, M. D. Green synthesis of silver nanoparticles: biomolecule-nanoparticle organizations targeting antimicrobial activity. *RSC Adv.* **2019**, *9* (5), 2673−2702.
(19) Tao, C. Antimicrobial activity and toxicity of gold nanoparticles: research progress, challenges and prospects. *Lett. Appl. Microbiol* **2018**, *67* (6), 537−543.
(20) Cui, Y.; Zhao, Y.; Tian, Y.; Zhang, W.; Lü, X.; Jiang, X. The molecular mechanism of action of bactericidal gold nanoparticles on Escherichia coli. *Biomaterials* **2012**, *33* (7), 2327−2333.
(21) Alon, U.; Surette, M. G.; Barkai, N.; Leibler, S. Robustness in bacterial chemotaxis. *Nature* **1999**, *397* (6715), 168−171.
(22) Zhao, Y.; Tian, Y.; Cui, Y.; Liu, W.; Ma, W.; Jiang, X. Small Molecule-Capped Gold Nanoparticles as Potent Antibacterial Agents That Target Gram-Negative Bacteria. *J. Am. Chem. Soc.* **2010**, *132* (35), 12349−12356.
(23) Kyzioł, A.; et al. Towards plant-mediated chemistry − Au nanoparticles obtained using aqueous extract of Rosa damascena and their biological activity in vitro. *J. Inorg. Biochem* **2021**, *214*, No. 111300.
(24) Rakus, K.; et al. Antiviral response of adult zebrafish (Danio rerio) during tilapia lake virus (TiLV) infection. *Fish Shellfish Immunol* **2020**, *101*, 1−8.
(25) Pfaffl, M. W. A new mathematical model for relative quantification in real-time RT-PCR. *Nucleic Acids Res.* **2001**, *29* (9), 45e−445.
(26) Widziolek, M.; et al. Gingipains protect Porphyromonas gingivalis from macrophage-mediated phagocytic clearance. *PLoS Pathog* **2025**, *21* (1), No. e1012821.
(27) Sati, A.; et al. From Past to Present: Gold Nanoparticles (AuNPs) in Daily Life−Synthesis Mechanisms, Influencing Factors, Characterization, Toxicity, and Emerging Applications in Biomedicine, Nanoelectronics, and Materials Science. *ACS Omega* **2025**, *10* (31), 33999−34087.
(28) Soltanmohammadi, F.; Gharehbaba, A. M.; Zangi, A. R.; Adibkia, K.; Javadzadeh, Y. Current knowledge of hybrid nanoplatforms composed of exosomes and organic/inorganic nanoparticles for disease treatment and cell/tissue imaging. *Biomedicine & Pharmacotherapy* **2024**, *178*, No. 117248.
(29) Esporrín-Ubieto, D.; Fraire, J. C.; Sánchez-deAlcázar, D.; Sánchez, S. Engineered Plasmonic and Fluorescent Nanomaterials for Biosensing, Motion, Imaging, and Therapeutic Applications. *Adv. Mater.* **2025**.
(30) Ghosh, S.; Solanki, R.; Bhatia, D.; Sankaranarayanan, S. Nanomaterials for delivery of medicinal plant extracts and phytochemicals: Potential applications and future perspectives. *Plant Nano Biology* **2025**, *12*, No. 100161.
(31) Parvin, N.; Aslam, M.; Joo, S. W.; Mandal, T. K. Nano-Phytomedicine: Harnessing Plant-Derived Phytochemicals in Nanocarriers for Targeted Human Health Applications. *Molecules* **2025**, *30* (15), 3177.
(32) Lithi, I. J.; Ahmed Nakib, K. I.; Chowdhury, A. M. S.; Sahadat Hossain, M. A review on the green synthesis of metal (Ag, Cu, and Au) and metal oxide (ZnO, MgO, Co 3 O 4, and TiO 2) nanoparticles using plant extracts for developing antimicrobial properties. *Nanoscale Adv.* **2025**, *7* (9), 2446−2473.
(33) Ribeiro, A. I.; Dias, A. M.; Zille, A. Synergistic Effects Between Metal Nanoparticles and Commercial Antimicrobial Agents: A Review. *ACS Appl. Nano Mater.* **2022**, *5* (3), 3030−3064.
(34) Nagime, P. V.; et al. Articulating the multifaceted application of bioactive compound decorated silver/gold nanoparticles: Current and future prospective. *Biocatal Agric Biotechnol* **2025**, *69*, No. 103776.
(35) Rao, P. R.; Seshadri, T. R. Constitution of Populnin. *Proceedings of the Indian Academy of Sciences - Section A* **1946**, *24* (5), 456.
(36) Cutler, R. R., "SECONDARY METABOLITES | Medicinal and Pharmaceutical Uses," in *Encyclopedia of Rose Science*; Elsevier, 2003; pp 716−726. doi: .
(37) Musial, C.; Kuban-Jankowska, A.; Gorska-Ponikowska, M. Beneficial Properties of Green Tea Catechins. *Int. J. Mol. Sci.* **2020**, *21* (5), 1744.
(38) Cendrowski, A.; Kraśniewska, K.; Przybył, J. L.; Zielińska, A.; Kalisz, S. Antibacterial and Antioxidant Activity of Extracts from Rose Fruits (Rosa rugosa). *Molecules* **2020**, *25* (6), 1365.
(39) Maželienė, Ž.; Kirvaitienė, J.; Kaklauskienė, K.; Volskienė, R.; Aleksandravičienė, A. Antifungal and Antibacterial Activity of Aqueous and Ethanolic Extracts of Different Rosa rugosa Parts. *Microbiol Res. (Pavia)* **2025**, *16* (1), 26.
(40) Gerasimova, T.; et al. Screening of Cytotoxic and Genotoxic Activities of Subcritical Water Extracts from R. damascena and R. alba Flowers. *Molecules* **2025**, *30* (21), 4294.
(41) Lalovski, I.; Krasteva, M.; Yordanov, E.; Hristov, E.; Dimitrov, M.; Parvova, I. Safety of active substances derived from Rosa damascena and their potential biological activity in humans: a systematic review. *Pharmacia* **2025**, *72*, 1−10.
(42) Majewska, L.; Dorosz, K.; Kijowski, J. Efficacy of Rose Stem Cell-Derived Exosomes (<scp > RSCEs</scp>) in Skin Treatment: From Healing to Hyperpigmentation Management: Case Series and Review. *J. Cosmet. Dermatol.* **2025**, *24* (1), No. e16776.
(43) Lueangarun, S.; Cho, B. S.; Tempark, T. Topical moisturizer with rose stem cell-derived exosomes (RSCEs) for recalcitrant seborrheic dermatitis: A case report with 6 months of follow-up. *J. Cosmet Dermatol* **2024**, *23* (10), 3128−3132.
(44) Majewska, L.; Kondraciuk, A.; Dorosz, K.; Budzyńska, A. Application of Standardized Rosa damascena Stem Cell-Derived Exosomes in Dermatological Wound Healing and Scar Management: A Retrospective Case-Series Study with Long-Term Outcome Assessment. *Pharmaceutics* **2025**, *17* (7), 910.
(45) Esfandiary, E.; et al. Novel effects of Rosa damascena extract on patients with neurocognitive disorder and depression: A clinical trial study. *Int. J. Prev Med.* **2018**, *9* (1), 57.
(46) Gholinezhad, Z.; Karimi, F. Z.; Rakhshandeh, H.; Mazloum, S. R. Impact of Rosa damascena extract on improving menopausal symptoms: A randomized clinical trial. *Adv. Integr Med.* **2025**, *12* (3), No. 100460.
(47) Liu, A.; et al. Rose bud extract as a natural antimicrobial agent against Staphylococcus aureus: Mechanisms and application in maintaining pork safety. *LWT* **2023**, *176*, No. 114527.
(48) Kulczyńska, J.; et al. Sustainable poly(vinyl alcohol)/chitosan electrospun nanofibers and casted films with bioactive additives − comparative study on physicochemical properties and in vitro biological activity. *Ind. Crops Prod* **2025**, *233*, No. 121335.
(49) El-Sherbiny, I. M.; Sedki, M. Green Synthesis of Chitosan-Silver/Gold Hybrid Nanoparticles for Biomedical Applications. *Pharm. Nanotechnol.* **2019**, 79−84.
(50) Volkov, D. A.; Zakharevich, A. A.; Chvalun, S. N.; Grigoriev, T. E. Silver Reduction in Aqueous Solutions of Chitosan with Different Molecular Weights. *Nanobiotechnology Reports* **2023**, *18* (S1), S116−S120.
(51) Wang, W.; et al. Anti-quorum sensing evaluation of methyleugenol, the principal bioactive component, from the Melaleuca bracteata leaf oil. *Front Microbiol* **2022**, *13*, No. 970520.
(52) Venkatramanan, M.; et al. Inhibition of Quorum Sensing and Biofilm Formation in *Chromobacterium violaceum* by Fruit Extracts of *Passiflora edulis*. *ACS Omega* **2020**, *5* (40), 25605−25616.

https://doi.org/10.1021/acsbiomaterials.5c01488
ACS Biomater. Sci. Eng. 2026, 12, 1508−1521

(53) Wang, S.; et al. Bacteriostatic Effect of Quercetin as an Antibiotic Alternative In Vivo and Its Antibacterial Mechanism In Vitro. *J. Food Prot* **2018**, *81* (1), 68−78.
(54) Nguyen, T. L. A.; Bhattacharya, D. Antimicrobial Activity of Quercetin: An Approach to Its Mechanistic Principle. *Molecules* **2022**, *27* (8), 2494.
(55) Willian de Alencar Pereira, E.; Fontes, V. C.; da Fonseca Amorim, E. A.; de Miranda, R. d. C. M.; Carvalho, R. C.; de Sousa, E. M.; Cutrim, S. C. P. F.; Alves Lima, C. Z. G. P.; de Souza Monteiro, A.; Neto, L. G. L.; et al. Antimicrobial effect of quercetin against Streptococcus pneumoniae. *Microb Pathog* **2023**, *180*, No. 106119.
(56) Wang, R.; Moon, S.-K.; Kim, W.-J.; Dhandapani, S.; Kim, H.; Kim, Y.-J. Biologically Synthesized *Rosa rugosa* -Based Gold Nanoparticles Suppress Skin Inflammatory Responses via MAPK and NF-κB Signaling Pathway in TNF-α/IFN-γ-Induced HaCaT Keratinocytes. *ACS Omega* **2022**, *7* (40), 35951−35960.
(57) Klekotko, M.; Matczyszyn, K.; Siednienko, J.; Olesiak-Banska, J.; Pawlik, K.; Samoc, M. Bio-mediated synthesis, characterization and cytotoxicity of gold nanoparticles. *Phys. Chem. Chem. Phys.* **2015**, *17* (43), 29014−29019.
(58) Olivier, M.; Hollstein, M.; Hainaut, P. TP53 Mutations in Human Cancers: Origins, Consequences, and Clinical Use. *Cold Spring Harb Perspect Biol.* **2010**, *2* (1), a001008−a001008.
(59) Laka, K.; Mbita, Z. P53-Related Anticancer Activities of Drimia calcarata Bulb Extracts Against Lung Cancer. *Front Mol. Biosci* **2022**, *9*, No. 876213.
(60) Yin, Y.; et al. Gold nanoparticles targeting the autophagy−lysosome system to combat the inflammation-compromised osteogenic potential of periodontal ligament stem cells: From mechanism to therapy. *Biomaterials* **2022**, *288*, No. 121743.
(61) Florance, I.; Cordani, M.; Pashootan, P.; Moosavi, M. A.; Zarrabi, A.; Chandrasekaran, N. The impact of nanomaterials on autophagy across health and disease conditions. *Cell. Mol. Life Sci.* **2024**, *81* (1), 184.
(62) Liu, P.-F.; et al. Map1lc3b and Sqstm1Modulated Autophagy for Tumorigenesis and Prognosis in Certain Subsites of Oral Squamous Cell Carcinoma. *J. Clin Med.* **2018**, *7* (12), 478.
(63) Ma, X.; et al. Gold Nanoparticles Induce Autophagosome Accumulation through Size-Dependent Nanoparticle Uptake and Lysosome Impairment. *ACS Nano* **2011**, *5* (11), 8629−8639.
(64) Zhou, H.; et al. Gold nanoparticles impair autophagy flux through shape-dependent endocytosis and lysosomal dysfunction. *J. Mater. Chem. B* **2018**, *6* (48), 8127−8136.
(65) Lubin, A.; et al. A versatile, automated and high-throughput drug screening platform for zebrafish embryos. *Biol. Open* **2021**, *10* (9), bio058513.
(66) Santoriello, C.; Zon, L. I. Hooked! Modeling human disease in zebrafish. *J. Clin. Invest.* **2012**, *122* (7), 2337−2343.
(67) Langheinrich, U.; Hennen, E.; Stott, G.; Vacun, G. Zebrafish as a Model Organism for the Identification and Characterization of Drugs and Genes Affecting p53 Signaling. *Curr. Biol.* **2002**, *12* (23), 2023−2028.
(68) van Soest, J. J.; Stockhammer, O. W.; Ordas, A.; Bloemberg, G. V.; Spaink, H. P.; Meijer, A. H. Comparison of static immersion and intravenous injection systems for exposure of zebrafish embryos to the natural pathogen Edwardsiella tarda. *BMC Immunol* **2011**, *12*, 58.
(69) Asharani, P. V.; lianwu, Y.; Gong, Z.; Valiyaveettil, S. Comparison of the toxicity of silver, gold and platinum nanoparticles in developing zebrafish embryos. *Nanotoxicology* **2011**, *5* (1), 43−54.
(70) Windell, D. L.; Mourabit, S.; Moger, J.; Owen, S. F.; Winter, M. J.; Tyler, C. R. The influence of size and surface chemistry on the bioavailability, tissue distribution and toxicity of gold nanoparticles in zebrafish (Danio rerio). *Ecotoxicol Environ. Saf* **2023**, *260*, No. 115019.
(71) Böhme, S.; et al. Metal uptake and distribution in the zebrafish (Danio rerio) embryo: differences between nanoparticles and metal ions. *Environ. Sci. Nano* **2017**, *4* (5), 1005−1015.
(72) Batir-Marin, D.; et al. Exploring Oxidative Stress Mechanisms of Nanoparticles Using Zebrafish (Danio rerio): Toxicological and Pharmaceutical Insights. *Antioxidants* **2025**, *14* (4), 489.
(73) Machado, S.; et al. Toxicity in vitro and in Zebrafish Embryonic Development of Gold Nanoparticles Biosynthesized Using Cystoseira Macroalgae Extracts. *Int. J. Nanomedicine* **2021**, *16*, 5017−5036.
(74) Plumet, L.; et al. The zebrafish embryo model: unveiling its potential for investigating phage therapy against methicillin-resistant *Staphylococcus aureus* infection. *Antimicrob. Agents Chemother.* **2024**, *68* (7), No. e00561-24.

https://doi.org/10.1021/acsbiomaterials.5c01488
ACS Biomater. Sci. Eng. 2026, 12, 1508−1521